Abstract submitted for presentation at the 10th WWWFB, Oxford, April 1995

NONLINEAR WAVE LOADS AND RUNUP UPON A SURFACE PIERCING CYLINDER

Pierre Ferrant
SIREHNA
Immeuble Atlanpole – 1 rue de la Noë – 44071 NANTES CEDEX 03 – FRANCE

A numerical solution method for the diffraction of nonlinear regular waves of permanent form by three dimensional bodies is proposed. The computation is based on a boundary integral equation method, with a mixed Euler–Lagrange approach for the time stepping. The method is an extension of a previously developed linear time domain computational model for free surface flows (Ferrant 1993). The behaviour of the nonlinear model was first tested on radiation and diffraction problems for submerged bodies, using a fully Lagrangian formulation for the free surface motion (Ferrant 1994). In the present paper, we report on the extension of the model to surface piercing bodies. While the solution of nonlinear diffraction problems on submerged bodies was based on a fully Lagrangian form of the free surface conditions (Ferrant 1994), the present model is based on a modified formulation in which free surface mesh points are fixed in their horizontal motion. This change was motivated by the resulting easier treatment of the free surface body intersection line as well as by the more straightforward implementation of interpolation and smoothing techniques. Numerical results are presented on the case of a bottom mounted vertical cylinder submitted to a nonlinear incident wave.

SOLUTION PROCEDURE

The core of the numerical model is composed of a boundary integral equation method coupled with a time marching scheme.

A boundary element method is used for the solution of the boundary integral equation formulation of the problem. The method is based on isoparametric triangular elements distributed over the different boundaries. A piecewise linear, continuous variation of the solution over the boundary is thus assumed, and collocation points are placed at panel vertices. At the intersection between solid boundaries and the free surface, both Neumann and Dirichlet conditions are specified, by keeping two collocation points at the same geometrical location. This discretization scheme reduces the integral equation to a linear algebraïc system to be solved for the normal velocity on Dirichlet boudaries (free surface) and the potential on Neumann boundaries. This system is made of the influence coefficients of linearly varying distributions of sources and dipoles on boundary elements. These coefficients are computed using analytical formulas for the near–field, and different approximate formulas for the intermediate and far–field. A preconditioned GMRES iterative scheme is used for the solution of linear systems of equations.

After solution of the boundary value problem, free surface conditions are integrated in time, which is the second step of the mixed Euler–Lagrange method. We presently use a fourth order Runge–Kutta scheme, with "frozen" coefficients, that is influence coefficients are updated only once per time step, while four solutions of the boundary value problem are performed. With

sufficiently small time steps, this approximation has no noticeable effect on the accuracy of the simulation, and results in significant savings of computer time.

The overall simulation strategy is the same as in the fully Lagrangian version. The incident wave is given by the stream function theory of Rienecker & Fenton (1981). This steady wave solution is used to prescribe the initial conditions, as well as the time dependent boundary conditions on the outer surface of the computational domain. At time t = 0, the potential and wave elevation given by the incident wave model are imposed on the whole boundary of the computational domain. The Neumann condition on the body is then progressively introduced, with a ramp over half a wave period. During the simulation, Neumann conditions given by the wave model are maintained on the vertical outer boundary. On the free surface surrounding the body, the original conditions are applied, while on the other part, up to the outer Neumann boundary an absorbing layer is introduced, in which the damping is applied only to the perturbation to the incident wave. This allows a smooth transition between the numerical solution on the free surface and the incident wave model imposed on the outer boundary.

The quality of free surface velocity and geometry computations is essential to the stability and accuracy of mixed Euler–Lagrange method. In the present formulation, bi–cubic splines are used for the interpolation of the potential and vertical coordinate at the free surface. These quantities are interpolated in radial and aximuthal directions, accounting for the axisymmetric geometry of the computational domain around the cylinder. Fluid velocities, tangential and normal vectors at the free surface are then computed directly from the spline coefficients. The spline representation along locally orthogonal coordinates also allows an easy implementation of smoothing formulas. In the following computation, five points Chebyshev formulas are applied in orthogonal directions at each free surface point. The smoothing occurs every five time steps.

NUMERICAL RESULTS

The numerical model has been applied to the solution of the nonlinear diffraction problem on a bottom mounted, surface piercing cylinder.

The cylinder radius is R/H = 0.862, where H is the water depth. The incident regular wave amplitude is A/H = 0.1, with wavelength $\lambda/H = 4.09$ and period $T = 5.23\sqrt{H/g}$. A computational domain of radius $R_D/H = 9$ is considered, and the mesh is composed of 4968 panels on the half domain, that is a total of 9936. A view of the domain in its initial configuration is given by figure 1. The diffracted wave field is absorbed by an annular absorbing zone of radius $Ra = \lambda$. The time step is dt = T/50, and the simulation was run over 320 time steps, that is more than six wave periods. In figure 2, we plot the horizontal force on the cylinder. A quasi steady state is observed after the end of the first period with only small variations of maxima and minima. Figures 3 and 4 give the wave heights at two different locations on the cylinder waterline, respectively at the weather side ($\theta = \pi$) and at the lee side ($\theta = 0$). These signals are also quite regular, despite on overshoot around $t\sqrt{g/H} = 15.$, after about three periods of simulation. The origin of this phenomenon is uncertain, but we believe that it is due to the influence of a partial reflection on the absorbing zone. Figure 5 is a view of the computational domain at an instant close to the maximum runup on the weather side of the cylinder.

CONCLUSION

We presented one of the first results obtained with the new version of our numerical model. Although a complete validation process is desirable, we consider that these preliminary results are very promissing and prove that fully nonlinear diffraction computations are now possible.

We intend now to undercome a validation of the model, by comparing nonlinear numerical results with existing higher order frequency domain results for small amplitudes, and with experimental data for higher incoming waves.

ACKNOWLEDGMENTS

The development of the code ANSWAVE is supported by the French Ministry of Defense, under contract DRET/SIREHNA 94/360. The application to nonlinear diffraction problems is part of a CLAROM project on "high frequency resonance of offshore structures", with BUREAU VERITAS, DORIS ENGINEERING, IFP, IFREMER, PRINCIPIA and SIREHNA as partners.

REFERENCES

P. FERRANT – "Threedimensional unsteady wave–body interactions by a boundary element method" – *Ship Technology Research, Vol. 40 n° 4, 165–175, 1993*

P. FERRANT – "Radiation and diffraction of nonlinear waves in three dimensions" – *BOSS'94 Conference, MIT, Cambridge, 1994*

MM. RIENECKER, J.D. FENTON – "A Fourier approximation method for steady water waves" *JFM 104, pp. 119–137, 1981*

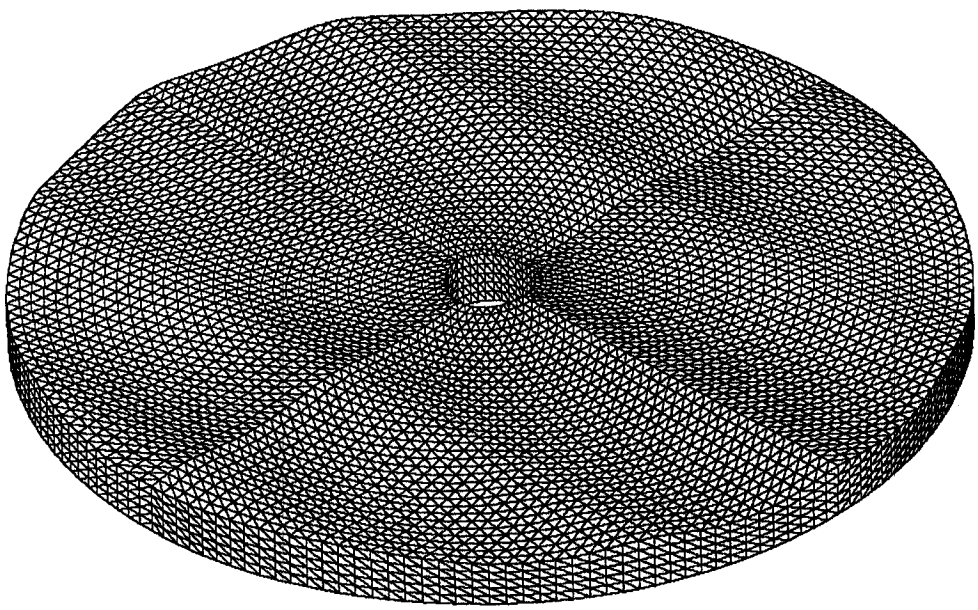

Figure 1 – Computational domain at t = 0

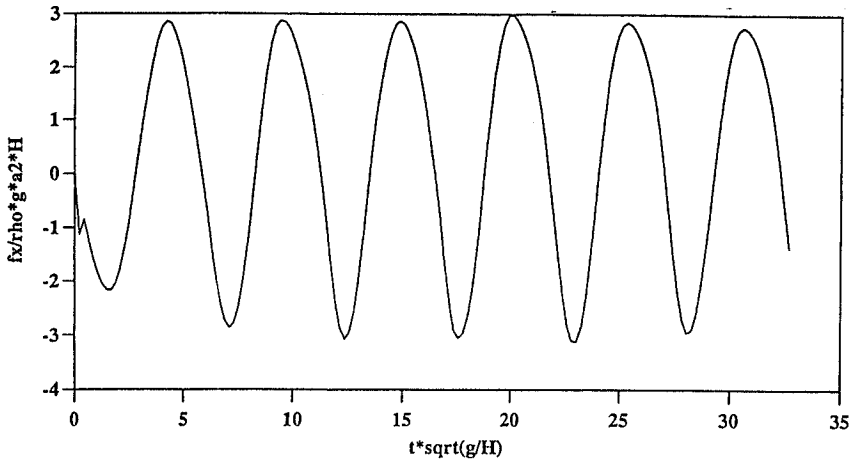

Figure 2 – Horizontal force on the cylinder

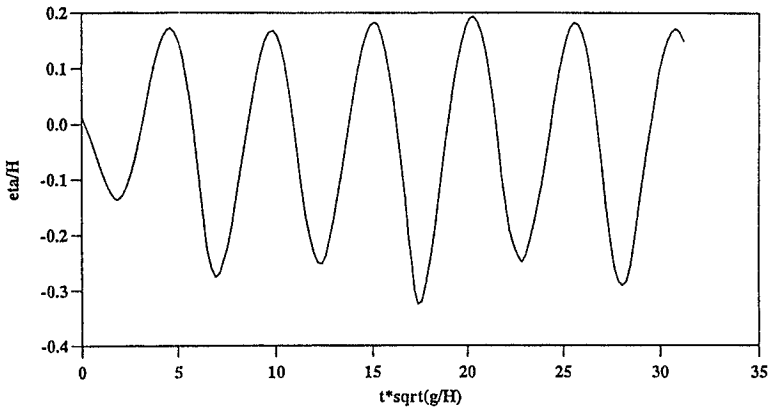

Figure 3 – Runup at upwave position

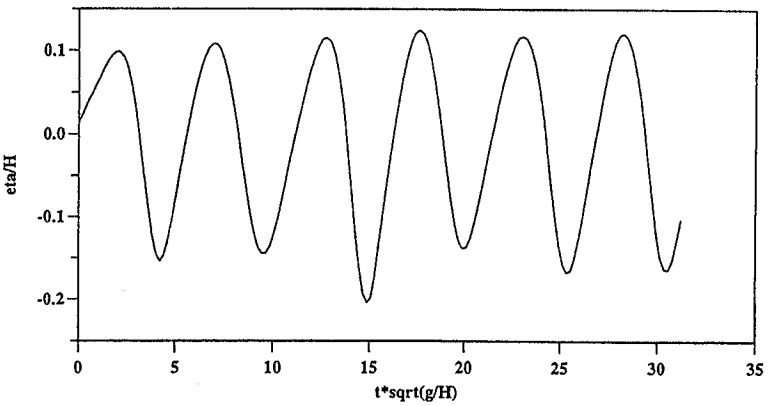

Figure 4 – Runup at downwave position

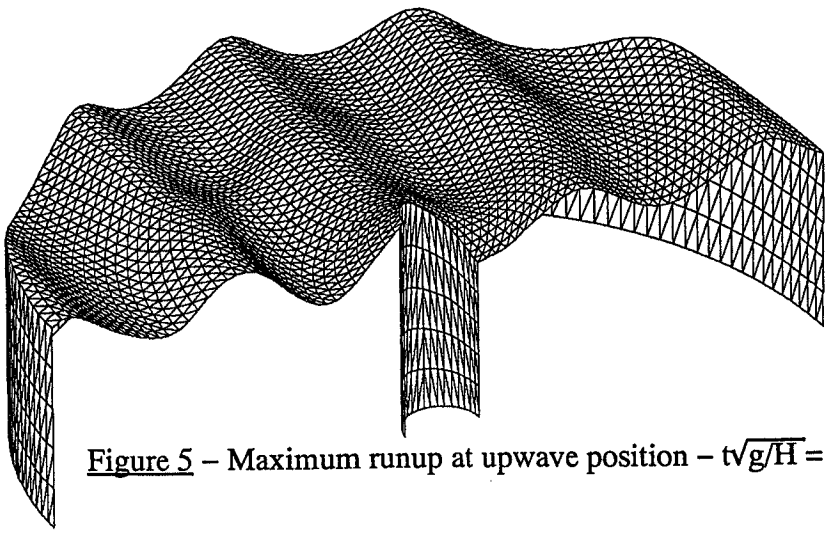

Figure 5 – Maximum runup at upwave position – $t\sqrt{g/H} = 30.78$